Site-Directed Mutagenesis of Histidine 238 in Mouse Adenosine Deaminase: Substitution of Histidine 238 Does Not Impede Hydroxylate Formation[†,‡]

Vera Sideraki,[§] David K. Wilson,[∥] Linda C. Kurz,[⊥] Florante A. Quiocho,[∥] and Frederick B. Rudolph*[,§]

Department of Biochemistry and Cell Biology and The Institute of Biosciences and Bioengineering, Rice University, Houston, Texas 77005, Howard Hughes Medical Institute and Department of Biochemistry, Baylor College of Medicine, One Baylor Plaza, Houston, Texas 77030, and Department of Biochemistry and Molecular Biophysics, Washington University School of Medicine, St. Louis, Missouri 63110

Received June 14, 1996; Revised Manuscript Received September 11, 1996[⊗]

ABSTRACT: His 238, a conserved amino acid located in hydrogen-bonding distance from C-6 of the substrate in the active site of murine adenosine deaminase (mADA) and postulated to play an important role in catalysis, was altered into an alanine, a glutamate, and an arginine using site-directed mutagenesis. The Ala and Glu substitutions did not result in changes of the secondary or tertiary structure, while the Arg mutation caused local perturbations in tertiary structure and quenched the emission of one or more enzyme tryptophans. Neither the Glu or Arg mutations affected substrate binding affinity. By contrast, the Ala mutation enhanced substrate and inhibitor binding by 20-fold. The most inactive of the mutants, Glu 238, had a k_{cat}/K_m 4×10^{-6} lower than the wild-type value, suggesting that a positive charge on His 238 is important for proper catalytic function. The Ala 238 mutant was the most active ADA, with a k_{cat}/K_m 2×10^{-3} lower than the wild-type value. NMR spectroscopy and crystallography revealed that this mutant is able to catalyze hydration of purine riboside, a ground-state analog of the reaction. These results collectively show that His 238 is not required for formation of the hydroxylate used in the deamination and may instead have an important electrostatic role.

Adenosine deaminase (ADA)[1] is an enzyme indispensable to the purine metabolic pathway and the maintenance of a competent immune system. ADA catalyzes the irreversible deamination of adenosine and 2′-deoxyadenosine to their respective inosine derivatives and ammonia with a rate enhancement of 2×10^{12} relative to the nonenzymatic reaction (Frick et al., 1987). The reaction is believed to be encounter-controlled (Kurz & Frieden, 1987; Kurz et al., 1992) with a k_{cat} of 375 s^{-1} and k_{cat}/K_m of 1.4×10^7 M^{-1} s^{-1} (Frick et al., 1987). In the past, a wealth of kinetic information on ADA offered a number of possibilities with regard to the mechanism of the reaction, the intermediates present, and the important catalytic residues. Deamination was suggested to proceed by direct water attack instead of a covalent intermediate between the enzyme and the substrate (Wolfenden et al., 1977; Kurz & Frieden, 1987). Formation of a tetrahedral intermediate was proposed to be rate-limiting (Wolfenden, 1969), and enzyme sulfhydryl groups were implicated in catalysis (Zielke & Suelter, 1971; Weiss et al., 1987; Kati & Wolfenden, 1989). Histidine and/or carboxylate residues were also thought to participate in the reaction (Kurz & Frieden, 1983; Weiss et al., 1987; Kati & Wolfenden, 1989), and there was evidence for protonation on N-1 by an enzyme acid (Kurz & Frieden, 1983; Weiss et al., 1987; Porter & Spector, 1993).

The crystal structure of the murine enzyme complexed to ground-state and transition-state analogs identified key aspects of the chemistry employed by the enzyme (Wilson et al., 1991; Wilson & Quiocho, 1993). To create the hydroxylate nucleophile, ADA utilizes a zinc metal cofactor. A catalytic water molecule becomes polarized by its interaction with the zinc; a nearby base, His 238, is favorably located for proton abstraction (Figure 1). Asp 295, a zinc ligand, orients the hydroxylate such that one of the oxygen lone pairs points to the direction of C-6 of the substrate. The hydroxylate is further stabilized through its interaction with the zinc and His 238. Nucleophilic attack on C-6 changes the carbon hybridization from sp^2 to sp^3 and reduces the double-bond character between N-1 and C-6. During the attack, N-1 is protonated by Glu 217, a key catalytic residue (Mohamedali et al., 1996). The electrophilicity of C-6 of the substrate is enhanced through the reduction of the purine ring electron density by hydrogen-bonding interactions between all available purine nitrogen lone pairs and key enzyme residues such as Asp 296 and Gly 184. These residues also have the important function of stabilizing the substrate in the ground state (Sideraki et al., 1996). The tetrahedral intermediate, bearing both a hydroxylate and an amino group on C-6, collapses to the products, ammonia and the enolate form of inosine. A required chemical step here is protonation of the leaving amino group by an enzyme

[†] This work was supported by Grant GM 42436 (F.B.R.) and GM 33851 (L.C.K.) from the National Institutes of Health, by Grant C-1041 (F.B.R.) from the Robert A. Welch Foundation, and in part by the Howard Hughes Medical Institute (F.A.Q.).

[‡] PDB ID codes for mutant ADA crystal structures H238A and H238E are 1UIO and 1UIP, respectively.

* Corresponding author: Dr. Frederick B. Rudolph, Department of Biochemistry and Cell Biology, Rice University, M.S. 140, 6100 Main St, Houston, TX 77005-1892. Tel: 713-527-4017. Fax: 713-285-5154. E-mail: fbr@rice.edu.

[§] Rice University.

[∥] Baylor College of Medicine.

[⊥] Washington University School of Medicine.

[⊗] Abstract published in *Advance ACS Abstracts,* November 1, 1996.

[1] Abbreviations: ADA, adenosine deaminase; mADA, murine adenosine deaminase; ss DNA, single-stranded DNA; IPTG, isopropyl β-D-thiogalactopyranoside; CD, circular dichroism; FAAS, flame atomic absorption spectroscopy; N^6MA, N^6-methyl adenosine; PR, purine riboside; HDPR, 6(*R*)-hydroxy-1,6-dihydropurine ribonucleoside.

S0006-2960(96)01427-4 CCC: $12.00

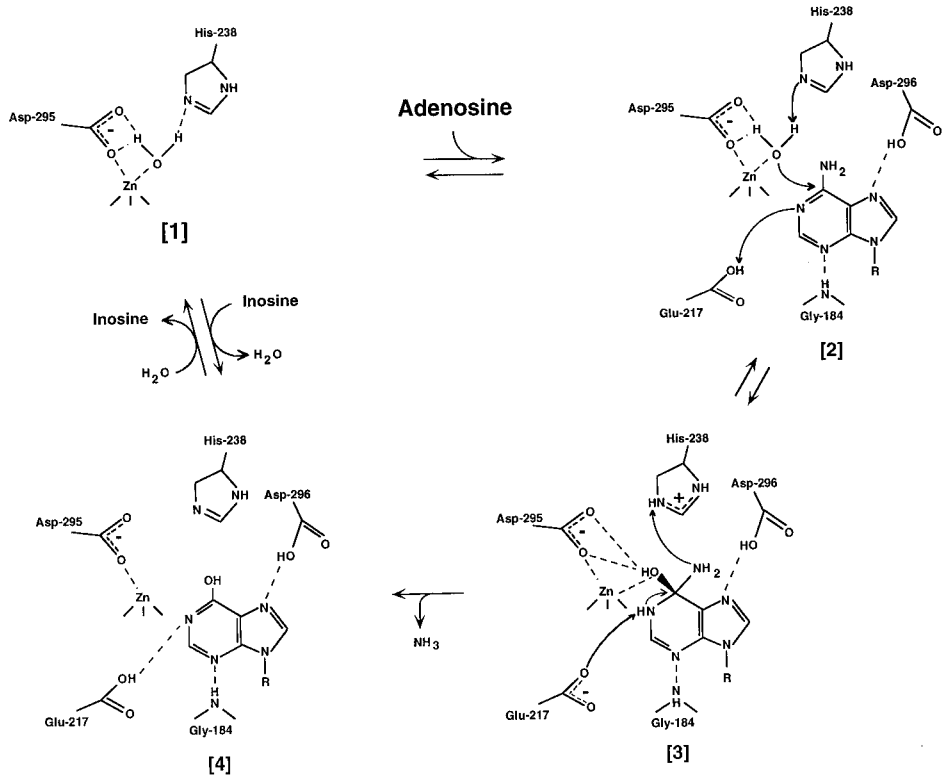

FIGURE 1: Schematic diagram of the proposed mechanism for the reaction catalyzed by adenosine deaminase. Dashed lines indicate noncovalent interactions between neighboring atoms. Step 1: The catalytic water is polarized through its interaction with the zinc cofactor and oriented for attack by hydrogen bonds to His 238 and Asp 295. Step 2: His 238 abstracts the proton from the catalytic water and the hydroxylate attacks C-6 of the substrate; the N-1−C-6 double bond is lost, and N-1 becomes protonated by Glu 217. Also shown are Asp 296 and Gly 184 donating hydrogen bonds to N-7 and N-3, respectively. Step 3: The tetrahedral intermediate collapses with the amino group becoming protonated, possibly by His 238, and leaving in the form of ammonia. Step 4: The enol form of the product inosine is shown bound to the active site.

acid. Neither of the two ADA crystal structures reveals probable proton donors, with the closest being Asp 295, at a distance of 3.2 Å, and His 238, at 4.5 Å. Another possibility is that solvent protonates the leaving group, as occurs in models of the reaction catalyzed by AMP deaminase (Kline & Schramm, 1996).

His 238 is a key residue in the above mechanism for the ADA-catalyzed deamination. It is proposed to be the base creating the attacking nucleophile, to orient and stabilize the hydroxylate for attack, and to possibly function as a proton donor to the leaving group. His 238 has been conserved in sequences from *Escherichia coli*, mouse, and human ADA enzymes (Chang et al., 1991). To investigate its proposed functions, three site-directed His 238 mutants, Ala 238, Glu 238, and Arg 238, were synthesized, purified, and characterized. Our results reveal that this conserved histidine is not required for proton abstraction from the catalytic water during formation of the hydroxylate. Moreover, this work suggests that this histidine may be important for catalysis by electrostatically stabilizing the hydroxylate via its positive charge.

MATERIALS AND METHODS

Bacterial Strains and Vectors. The mouse adenosine deaminase cDNA was inserted in the pRC4 phagemid expression vector under control of an IPTG-inducible tac promoter as described before (Mohamedali et al., 1996). *E. coli* strains CJ236 and BW313 (genotype *dut*$^-$*ung*$^-$) were used for the production of uridine-rich ss DNA. A third *E. coli* strain, 71-18, was used for mutant selection and plasmid propagation. Wild-type and mutant plasmids were expressed in the ADA$^-$ strain SΦ3834 (Chang et al., 1991). This strain contains a deletion of the adenosine deaminase (*add*) gene and two neighboring genes. Both the pRC4 vector and the SΦ3834 strain were developed in Dr. Rodney Kellems' laboratory at Baylor College of Medicine, Houston.

Site-Directed Mutagenesis. The Kunkel method for producing site-specific mutants was used (Kunkel et al., 1987). Uridine-rich ss DNA was isolated from pRC4-transformed CJ236/BW313 cells (*dut*$^-$*ung*$^-$ genotype). The following mutagenic primers (with the codon for residue 238 in bold) were designed for annealing onto the template ss DNA based on the sequence information for mouse ADA: Ala 238, 5′ GGT GTG ATA ACC **CGC** TCC CAC CCT CTC 3′; Arg 238, 5′ GGT GTG ATA ACC **ACG** TCC CAC CCT CTC 3′; Glu 238, 5′ GGT GTG ATA ACC **TTC** TCC CAC CCT CTC 3′.

The second strand was synthesized using the Muta-Gene M13 *in vitro* mutagenesis kit (Bio-Rad). The synthesized double-stranded DNA products were transformed into a wild-type strain (71-18) and selected on ampicillin-containing plates. ss DNA from individual colonies was isolated and sequenced in the area of the mutation (sequenase kit, United States Biochemicals). Once mutant colonies were identified (only 15−25% of all colonies), the entire cDNA was sequenced to ensure its integrity.

Protein Expression and Purification. Mutant and wild-type ADA proteins were expressed and purified from SΦ3834 as described elsewhere (Sideraki et al., 1996). The His 238 mutant enzymes eluted at similar times to the

wild-type ADA. Dot blots were used to identify mutants with low activity (H238A, H238E). Purified proteins were stored in Tris-Zn buffer (10 mM Tris-HCl, pH 7.0, 10 μM zinc sulfate, 50% glycerol, 1 mM dithiothreitol) in air-tight vials under argon at −20 °C.

SDS−Polyacrylamide Gel Electrophoresis, Western Blots, and Dot Blots. SDS−polyacrylamide gel electrophoresis was performed according to the method of Laemmli (1970) on a minigel apparatus (Bio-Rad). Proteins were stained with Coomassie brilliant blue. The Rainbow molecular weight markers (Amersham Corp.) were used as standards. Western blots and dot blots were performed as described before (Mohamedali et al., 1996) using goat anti-mADA polyclonal IgG as the primary antibody and alkaline phosphatase-conjugated rabbit anti-goat IgG as the secondary antibody (Sigma Immunochemicals). Protein concentrations were determined by the method of Bradford (1976) using bovine serum albumin as standard and the Bio-Rad protein assay reagent.

Enzyme Assays and Kinetic Analyses. Enzymatic activities were assayed on a Cary 118 spectrophotometer by measuring the rate of ADA-dependent increase of inosine absorption at 235 nm at 30 °C, using an extinction coefficient of 3.5 mM^{-1} cm^{-1}. For H238A, which has a much lower K_m value than the wild-type enzyme, the rate of ADA-dependent decrease of adenosine absorption was measured at 265 nm at 30 °C, using an extinction coefficient of 8.4 mM^{-1} cm^{-1}. One unit of ADA activity is defined as the amount of enzyme that produces 1 μmol of inosine/min. Cuvettes of 1 cm path length were used. Assays were carried out in 50 mM potassium phosphate buffer, pH 7.2. Activities were measured over at least six different concentrations of adenosine, and the assays were repeated at least three times. Adenosine concentrations ranged from 0.5 to 5 × K_m.

The concentration of enzyme in the assay mixture ranged from 0.1 nM for the wild-type to 0.2 μM for H238R and 0.3 μM for H238A and H238E. Kinetic parameters were determined by Lineweaver−Burk plots with a fourth power weighting function using the Enzyme Kinetics (Trinity Software) program. K_i values for two ADA inhibitors, N^6-methyladenosine (N^6MA) and purine riboside (PR), were determined for the enzymes. Assays were performed as above, with thorough mixing of the substrate and inhibitor in the reaction mixture prior to addition of the enzyme. Two to four different inhibitor concentrations bracketing the K_i value were used in the assays, and each velocity vs substrate curve was determined at least three times. Inhibition plots and K_i values were obtained as described above. The kinetic parameters K_m and k_{cat} refer to the following mechanism for a one-substrate reaction:

$$E + A \underset{k_{-1}}{\overset{k_1}{\rightleftharpoons}} EA \xrightarrow{k_2} E + P$$

where A is adenosine, E is ADA, and $K_m = (k_{-1} + k_2)/k_1$.

pH Dependence of the Reaction Catalyzed by ADA. pH profiles for the reaction catalyzed by the mutant and wild-type enzymes were determined over the range of pH 4−10 using the following buffers: 50 mM sodium acetate (pH 4, 5.5), 50 mM potassium phosphate (pH 7.0), and 50 mM glycine (pH 8.5, 10). The ionic strength of each buffer was adjusted to 0.1 with potassium sulfate. Reaction rates were measured by performing the enzyme assays in triplicate in each buffer at five different substrate concentrations.

Flame Atomic Absorption Spectroscopy. Flame atomic absorption spectroscopy (FAAS) was performed as described before (Sideraki et al., 1996) on a Perkin-Elmer 2380 atomic absorption spectrophotometer at the laboratory of Dr. David Giedroc, Texas A&M University, College Station, TX.

Circular Dichroism Spectroscopy. CD spectra were measured in the far-UV (200−260 nm) and the near-UV (250−340 nm) regions on an Aviv 6100 spectrometer. Measurements were made using a 0.02 cm path length cuvette (Starna Cells, Inc.). Each scan was recorded in 1 nm increments at 25 °C, repeated three times, and averaged. The proteins were in 20 mM Hepes buffer, pH 7.0, and their concentration was adjusted to 1 mg/mL (25 μM) prior to spectral acquisition. Protein concentration assays were used to determine the exact amount of enzyme in each sample. The spectrum of the buffer was subtracted from all protein spectra, and the observed ellipticities, θ, were normalized for protein concentration. The observed signal was converted to ellipticity from the formula $[\theta] = 10[\theta]_{obs}/cl$, where $[\theta]$ is the ellipticity measured in degrees, c is the protein concentration in mol/L, and l is the optical path length of the cell in dm. The final ellipticity is reported in deg dm^{-1} mM^{-1}.

Fluorescence Spectroscopy. Fluorescence spectroscopy was performed on a SLM 8100 spectrofluorimeter. The excitation wavelength was 290 nm, and the emission was scanned from 300 to 400 nm every 1 nm. Measurements were made using a 1 cm path length fluorescence cuvette (Starna Cells, Inc.). Samples of 25 μM ADA were in 20 mM Hepes buffer, pH 7.0. All spectra were normalized for protein concentration. The ∼40% quench in the intrinsic fluorescence of ADA caused by binding of the inhibitor (*R*)-deoxycoformycin was used to carry out stoichiometric active site titrations with two of the mutants, H238E and H238R, following the method of Kurz et al. (1985).

Crystallography. Crystals for two of our mutants, H238A and H238E, were successfully grown in the presence of purine ribonucleoside as described before (Wilson et al., 1991). Crystals were briefly harvested into a solution of 7.5% (w/v) poly(ethylene glycol) 6000, 35 mM sodium citrate, 1 mg/mL purine riboside, 30% (v/v) glycerol, pH 4.2. Room temperature crystals were very unstable when exposed to X-rays, so crystals were flash-frozen in a −150 °C nitrogen stream delivered by an Enraf-Nonius crystal cooler. The entire datasets were collected from single crystals of each mutant on an ASDC multiwire area detector. Data collection statistics for the mutant structures appear in Table 3.

Crystals of both mutants were isomorphous with those of the wild-type enzyme complexed with HDPR. The starting model for each mutant was therefore the structure of the wild-type protein with the inhibitor removed and a glycine replacing the histidine at the 238 position. After refinement of this modified structure, difference maps were used to determine the conformation of the side chain and the nature of the inhibitor (HDPR vs PR), as well as the location of water molecules in and around the active site. The model was modified accordingly and further refinement yielded the final model. Refinement statistics are shown in Table 3.

NMR Spectroscopy. Samples were diafiltrated extensively against 50 mM potassium phosphate buffer, pH 7.50, in a

stirred 10 mL Amicon cell equipped with a PM-10 membrane and a 800 mL reservoir. The enzyme sample was exchanged in D_2O buffer by repeatedly concentrating the sample to less than 0.5 mL and rediluting to 3 mL with fresh buffer in a previously rinsed Amicon Centricon-10 centrifuge concentrator. Three cycles were done with 99.9% D_2O buffer, and three were done with 99.996% D_2O buffer.

Actual enzyme concentrations were measured by active site titration with deoxycoformycin as previously described (Kurz et al., 1985), since the use of phosphate buffer for these experiments resulted in some loss of active enzyme as a consequence of zinc loss.

Conventional proton-decoupled ^{13}C NMR spectra were obtained at 150.7 MHz using a Varian Unity 600 spectrometer equipped with a 5 mm direct detect multinuclear probe. Broad-band proton-decoupled spectra were obtained using Waltz-16 decoupling. The temperature of the sample was 10 °C. The sample buffer was 50 mM potassium phosphate buffer, pH 7.50, in 99.996% D_2O and 0.15 M acetonitrile (as internal chemical shift standard). The cyano resonance of the standard was assigned the value of 118.9 ppm.

Since we anticipated the possibility that purine riboside may be bound to mutant enzymes in more than one form with varying occupancies, it was necessary to establish unambiguously that a given ^{13}C resonance was *J*-coupled to a single proton. A heteronuclear correlation (HMQC) experiment was performed to determine the chemical shift(s) of the single proton attached to ^{13}C of purine riboside and to confirm that a putative proton resonance was *J*-coupled to a ^{13}C resonance of appropriate value. One- and two-dimensional HMQC spectra were collected using a Varian Unity 500 spectrometer equipped with a Nalorac 5 mm triple-resonance indirect detection probe operating at 499.9 MHz on the proton channel and 125.7 MHz on the carbon channel. During the acquisition time of the HMQC experiment, continuous wave decoupling was applied at the carbon frequency identified in the one-dimensional direct detect spectrum. A coupled spectrum was also collected under the same conditions.

RESULTS

Purification of His 238 Mutants. After the presence of each of the three site-specific changes in the mADA cDNA was verified by sequencing, the mutant proteins were expressed in an ADA-deficient *E. coli* strain and purified to homogeneity (Figure 2). Throughout the purification process, the three mutant proteins behaved similarly to wild-type ADA. However, their average yields were lower (H238A, 70 mg; H238E, 50 mg; and H238R, 20 mg of protein per purification) than those of wild-type ADA (100 mg of protein obtained on average). Western blots of proteins from purified inclusion bodies revealed that 70−90% of the H238R and H238E mutants and 20% of the H238A mutant were found in inclusion bodies, compared to 10% of wild-type ADA (data not shown).

Evaluation of Secondary Structure and Zinc Content of His 238 Mutants. To examine whether the mutations at position 238 disrupted the enzyme's secondary structure, the far-UV circular dichroism spectra of His 238 mutants were compared to the wild-type spectrum. Wild-type murine ADA has a parallel α/β-barrel motif with eight central β-strands and eight peripheral α-helices and five additional

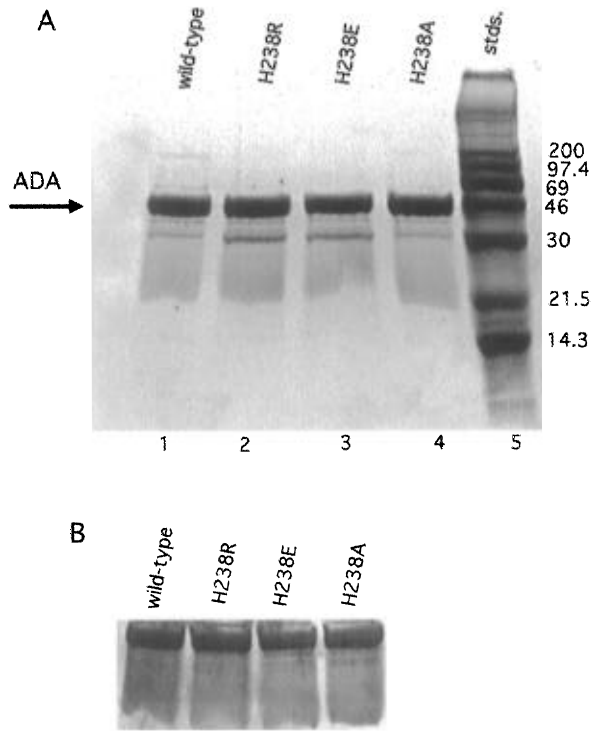

FIGURE 2: SDS−PAGE and Western blot of purified H238 mutants and wild-type ADA. Panel A: SDS−PAGE of adenosine deaminases: lane 1, wild-type; lane 2, H238R; lane 3, H238E; lane 4, H238A; lane 5, Rainbow molecular standards. The 39.9 kDa ADA band is designated by the arrow. Some amount of impurity is seen below the main band; most of it reacts with the anti-ADA antibody (panel B) and represents a degradation product of ADA. Approximately 12 μg of protein was loaded in each lane. Panel B: Western blot of an identical protein gel with the one shown in panel A using anti-ADA antibody. The main band is ADA; lower bands probably represent degradation products.

helices (Wilson et al., 1991). The CD spectrum of wild-type mADA exhibits a minimum at 222 nm characteristic of α-helical content and a minimum at 218 nm reflecting β-sheet structure (Adler et al., 1973). The CD spectra of all three ADA mutants are very similar to that of the wild-type (Figure 3). To evaluate the zinc content of wild-type and mutant ADA enzymes, flame atomic absorption spectroscopy measurements were performed after exhaustive dialysis of the samples against metal-free HEPES buffer. The results show that the three His 238 mutants contain wild-type amounts of zinc (data not shown). Thus, neither the secondary structure nor the zinc content of ADA were affected by mutations in residue 238.

Evaluation of ADA Tertiary Structure by Near-UV Circular Dichroism and Fluorescence Spectroscopies. Murine ADA contains 13 phenylalanine, 14 tyrosine, and 4 tryptophan residues (Yeung et al., 1985). The environment around the aromatic residues can be probed by the use of near-UV circular dichroism spectroscopy; additionally, the environment around the tryptophans can be examined by the use of fluoresecence spectroscopy. Figure 4 shows the near-UV CD spectra for His 238 mutants and wild-type ADA. The wild-type ADA spectrum in this region is very complex, due to contributions of the multiple Phe, Tyr, and Trp residues, as well as His and Cys residues. The spectra of H238A and H238E superimpose well with that of wild-type ADA, suggesting that the environment around the various aromatic residues has not been severely perturbed as a consequence of the Glu or Ala mutation. The Arg mutation,

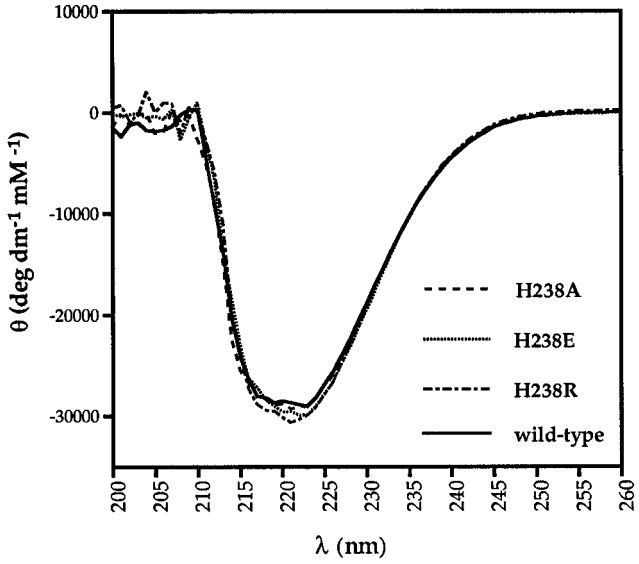

FIGURE 3: Far-UV circular dichroism spectra of His 238 mutants and wild-type ADA. Samples were at 1 mg/mL in 20 mM Hepes buffer, pH 7.0. Each spectrum shown represents the average of three scans. Little difference is seen in the secondary structure between mutants and wild-type. Minimum at 222 nm arises from α-helical structure and minimum at 218 nm from β-sheet.

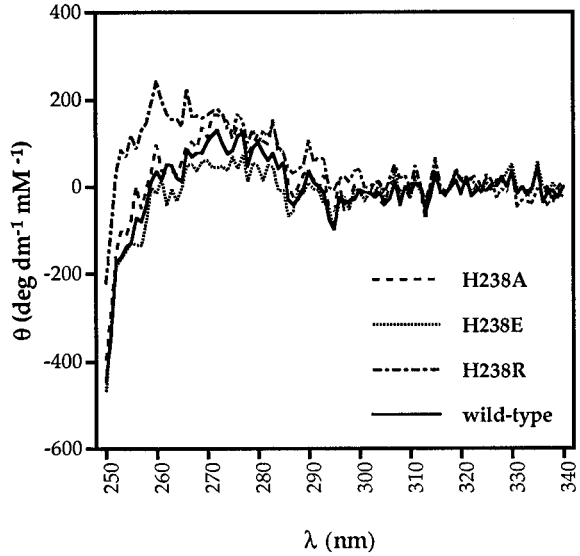

FIGURE 4: Near-UV circular dichroism spectra of His 238 mutants and wild-type ADA. Samples were at 1 mg/mL in 20 mM Hepes buffer, pH 7.0. Each spectrum shown represents the average of three scans. No major differences are noticeable in the spectra of H238A, H238E, and wild-type. The H238R spectrum, however, is altered in the 250−270 nm region, where contributions from all aromatic amino acids and histidines can be found.

however, has resulted in an altered near-UV CD spectrum, especially in the region 250−270 nm. Aromatic amino acids such as Phe, Tyr, and Trp as well as histidines can contribute to the ellipticity in this region (Vuilleumier et al., 1993; Freskard et al., 1994).

This first indication that an arginine at position 238 may have perturbed the tertiary structure of the molecule in the vicinity of aromatic residues was confirmed by fluorescence spectroscopy. Figure 5 shows the tryptophan emission fluorescence spectra for the three His 238 mutants and wild-type ADA. Murine ADA contains four tryptophans, which are mostly buried within the molecule; only two are relatively near the active site, Trp 264 and Trp 272 (Wilson et al.,

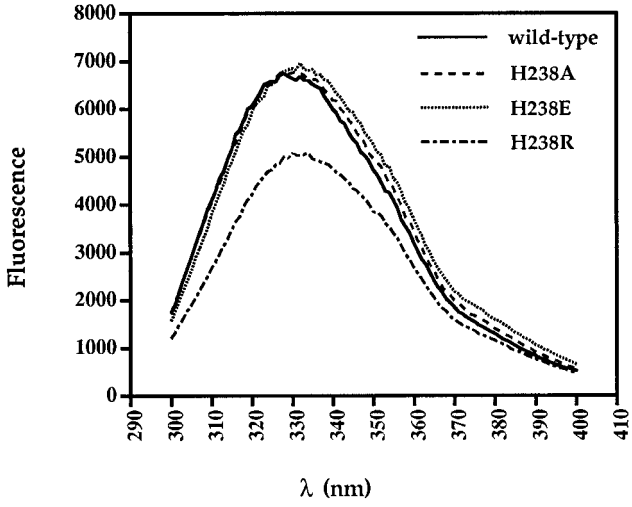

FIGURE 5: Tryptophan emission fluorescence spectroscopy of wild-type murine ADA and His 238 mutants. The excitation wavelength was 290 nm, and emission was scanned from 300 to 400 nm. Protein concentrations were 25 μM in 20 mM Hepes buffer, pH 7.0. The above spectra were normalized for protein concentration differences. H238A, H238E, and wild-type ADA have similar emission spectra with emission maxima at 328−332 nm. The H238R tryptophan emission intensity is quenched by 25%, and the emission maximum is shifted to 333 nm due to changes in the environment surrounding tryptophan residues as a result of the Arg mutation.

1991). Wild-type murine ADA emission has a maximum at 328 nm, compared to the emission maxima of the calf (340 nm) and human (335 nm) enzymes (Kurz et al., 1985; Philips et al., 1989). The spectrum of H238A is superimposable with that of the wild-type protein, with a maximum at 331 nm. The spectrum of H238E is similar in intensity but slightly red-shifted, with a maximum at 332 nm. The fluorescence spectrum from H238R differs markedly, however, with its tryptophan emission quenched by 25% with respect to the wild-type and a maximum at 333 nm. This result suggests that substitution of His 238 by the bulkier arginine has quenched the fluorescence emission of one or more of the enzyme's Trp components, perhaps by exposing them more to solvent. By contrast, neither the alanine nor the glutamate at position 238 have significantly perturbed tryptophan emission. Both the near-UV CD and fluorescence data suggest that neither an Ala nor a Glu at position 238 alter the tertiary structure of ADA, whereas a bulkier Arg substitution perturbs enzyme structure in the vicinity of certain aromatic residues.

Effects of His 238 Substitutions on Substrate and Inhibitor Binding and Catalysis. To examine the effects of the His 238 mutations on the kinetic behavior of ADA, the steady-state kinetic parameters for the wild-type and mutant enzymes were determined (Table 1). Murine ADA is a remarkably efficient enzyme, with a k_{cat}/K_m value in the order of 1×10^7 M^{-1} s^{-1}. This value compares well to the calf (Kurz et al., 1992) and human ADA (Bhaumik et al., 1993) values. The K_m value for adenosine is approximately 20 μM; the inhibition constants for two adenosine analogs (purine riboside and N^6-methyladenosine), both competitive inhibitors of the reaction, are slightly lower, at approximately 10 μM. The rate enhancement ADA affords compared to the nonenzymatic deamination of adenosine is 2×10^{12} (Frick et al., 1987). Changing the His 238 residue to Ala, Glu, or Arg dramatically reduces the efficiency of ADA as an enzyme. The most inactive of the three mutants is H238E,

Table 1: Steady-State Kinetic Parameters of His 238 Mutants and Wild-Type ADA[a]

sample	K_m[b] (μM)	k_{cat}[b] (s^{-1})	k_{cat}/K_m (μM^{-1} s^{-1})	K_i[b] (μM) PR	K_i[b] (μM) N^6MA
wild-type	21 ± 2	240 ± 20	11	9 ± 2	12 ± 1
H238A	1.0 ± 0.2	0.020 ± 0.001	0.020	50 ± 20	1.0 ± 0.2
H238E	29 ± 6	0.0010 ± 0.0001	0.00004	ND[c]	ND[c]
H238R	24 ± 2	0.17 ± 0.01	0.007	19 ± 4	10 ± 2

[a] Assays were performed at 30 °C in 50 mM phosphate buffer, pH 7.2, with adenosine as the substrate (see Materials and Methods). [b] Averages of at least three separate determinations. [c] Not determined.

with a k_{cat}/K_m value 4×10^{-6} lower than that of the wild-type. The most active of the three is H238A, with a k_{cat}/K_m value 2×10^{-3} that of the wild-type; H238R is intermediate between the other two mutants, with a k_{cat}/K_m value 6×10^{-4} that of the wild-type.

Neither the glutamate nor the arginine mutation affect the affinity of the enzyme for its substrate adenosine or the two competitive inhibitors (Table 1). The unchanged K_m and K_i values for H238R suggest that despite tertiary structure differences, the mutant has an intact active site, able to bind substrate or inhibitor with wild-type affinity. While H238E is too inactive to permit measurement of the inhibition constants, H238R is competitively inhibited by both PR and N^6MA, with a slightly increased K_i value of 19 μM for PR and a value of 10 μM for N^6MA.

The ability of the H238E and H238R mutant enzymes to bind substrates and inhibitors with wild-type affinity was also examined by performing active site titrations using stoichiometric amounts of the tight-binding inhibitor (*R*)-deoxycoformycin. Both mutants were able to bind the inhibitor at a 1:1 stoichiometry (data not shown). This result illustrates that the K_m and K_i values of the two mutants indeed reflect their ability to bind adenosine or adenosine analogs and do not arise from a chance wild-type contamination.

The undiminished substrate or inhibitor affinities exhibited by the Glu 238 and Arg 238 mutants support the proposed minimal role of His 238 in substrate binding (Wilson et al., 1991). It was surprising, therefore, that the alanine substitution had a major effect on substrate affinity, causing it to increase 20-fold relative to the wild-type. Thus, this mutant has a K_m of 1 vs 21 μM for adenosine and a K_i value for N^6MA of 1 μM versus the wild-type value of 12 μM. By contrast, purine riboside does not inhibit binding of adenosine as effectively in this mutant as it does in wild-type ADA, having a K_i value of 50 vs 9 μM.

The kinetic results with the H238E and H238R mutations suggest that substitution of His 238 causes a profound decrease in the catalytic activity of ADA, as expected from the postulated role of this residue in the mechanism. Results with H238A, however, also suggest that His 238 may interact with the substrate by destabilizing it in the ground state.

pH Dependence of Kinetic Parameters. In order to examine whether mutations of an active site residue like His 238 produced alterations in the pH dependence of catalysis, steady-state kinetic parameters for H238A, H238R, and wild-type ADA were determined in buffers of various pH values. For the two mutants and wild-type ADA, control experiments showed that the decrease in catalytic activity at the extremes of the pH range was not caused by irreversible enzyme denaturation (data not shown). In wild-type ADA, values of k_{cat} and k_{cat}/K_m are maximal at pH 7 and decrease on either side of this pH value in a bell-shaped curve with an acidic pK_a at approximately 5.5 and a basic one at 8.5 (Figure 6). Similar behavior is exhibited by the H238R mutant, although its k_{cat}/K_m and, more markedly, k_{cat} values decrease at acidic pH more rapidly than do the wild-type kinetic parameters. The catalytic process in the H238A mutant exhibits a very different pH dependence. The mutant k_{cat} value is now maximal at pH 5.5 rather than at pH 7.0. Its k_{cat}/K_m value is, within experimental error, also maximal at pH 5.5 but decreases sharply at basic pH values above 8.5. Both the substrate affinity of the H238A mutant for adenosine and its inhibition constant for N^6MA are slightly lower at pH 5.5 compared to at pH 7.0 (Table 2). These results demonstrate that replacement of His 238 by alanine considerably affects the pH dependence of the ADA-catalyzed reaction.

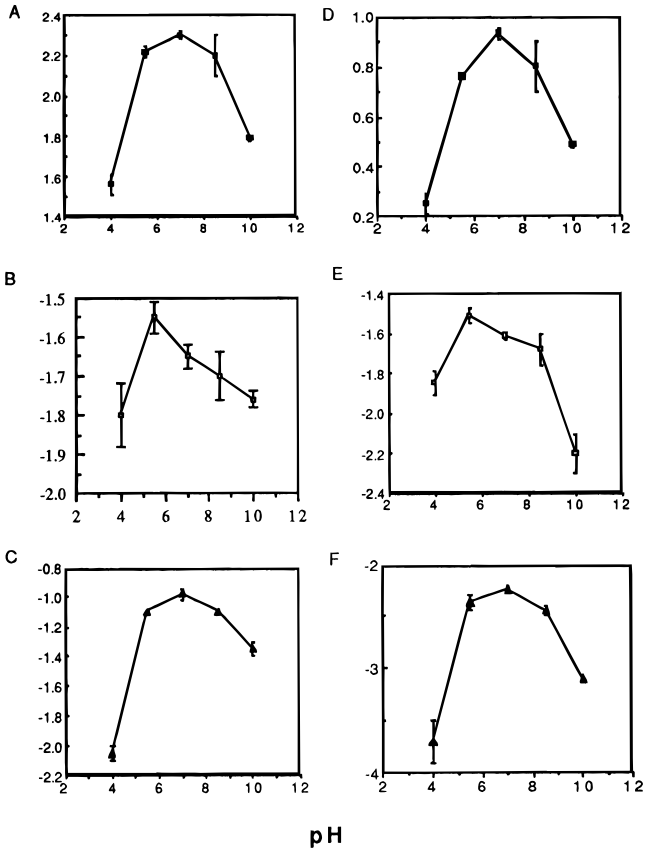

FIGURE 6: pH dependence of the steady-state kinetic parameters of H238A, H238R, and wild-type ADA: (A−C) log k_{cat} versus pH for (A) wild-type, (B) H238A, and (C) H238R; (D−F) log k_{cat}/K_m versus pH for (D) wild-type, (E) H238A, and (F) H238R.

Table 2: Steady-State Kinetic Parameters for H238A and Wild-Type ADA at pH 7.0 and pH 5.5

sample		K_m (μM)	k_{cat} (s−1)	k_{cat}/K_m (μM^{-1} s^{-1})	K_i PR (μM)
wild-type,	pH 5.5[a]	29 ± 2	166 ± 30	5.7	5 ± 2
	pH 7.0[b]	24 ± 2	200 ± 20	8.5	7 ± 2
H238A,	pH 5.5[a]	0.87 ± 0.08	0.028 ± 0.002	0.032	32 ± 1
	pH 7.0[b]	0.95 ± 0.06	0.024 ± 0.001	0.025	45 ± 10

[a] Assays were performed at 30 °C in 50 mM sodium acetate, pH 5.5. [b] Assays were performed at 30 °C in 50 mM phosphate buffer, pH 7.0.

Crystal Structures of H238A and H238E. The crystal structures of two His 238 mutants, H238A and H238E, were solved to 2.4 Å resolution and compared to the previously

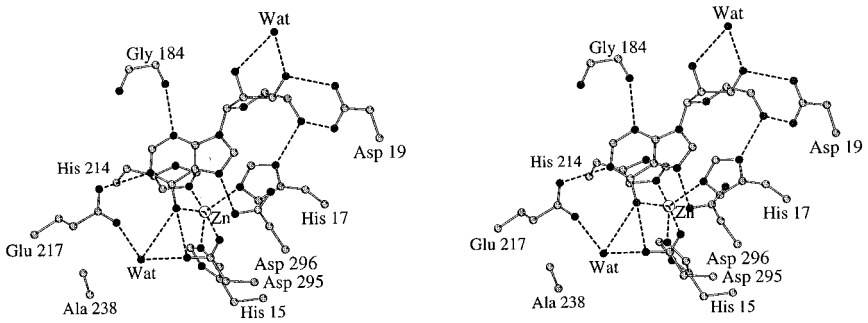

FIGURE 7: Model of the H238A active site. Purine riboside used in the crystallization has been converted to the hydrated analog, HDPR. Noncovalent interactions between atoms are represented by the dotted lines. The engineered Ala is shown at position 238; part of this site has been filled by a new water molecule adjacent to Ala 238. Its oxygen is at a distance of 3.4 Å from the C-6 OH of the HDPR analog. This model was created using the program MOLSCRIPT (Kraulis, 1991).

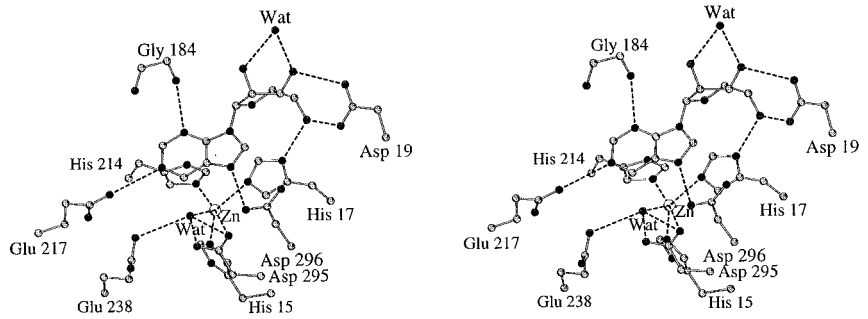

FIGURE 8: Model of the H238E active site bound to PR. Noncovalent interactions between atoms are represented by the dotted lines. The engineered Glu is shown at position 238. The zinc-water is coordinated to the zinc cofactor but has not attacked on C-6 of the bound inhibitor to form the hydrated adduct. This model was created using the program MOLSCRIPT (Kraulis, 1991).

solved structure of the wild-type enzyme complexed to HDPR, a transition-state analog (Wilson et al., 1991). Crystals were grown in the presence of PR, a substrate analog and inhibitor of the enzyme, which is hydroxylated to yield HDPR in the adenosine deaminase active site. The overall structures of the mutants showed few deviations between α-carbons or differences in zinc coordination when overlapped with the wild-type structure. Since His 238 does not directly interact with zinc in the wild-type structure, it was not surprising that a zinc atom was found in both mutant proteins. This result confirmed the previous observation that His 238 mutations do not decrease ADA's affinity for zinc. In the H238A structure, components of the active site other than residue 238 are situated similarly to the wild-type structure. An important difference, however, between this and the wild-type active site is the presence of a new water molecule occupying the space vacated by the imidazole ring of the histidine. As shown by the model of the H238A active site in Figure 7, the alanine substitution leaves enough room for a water molecule to fit. The distance between the oxygen of this water and the oxygen of the C-6 OH of HDPR is 3.43 Å, somewhat long for a hydrogen-bonding interaction. The most important feature revealed by the H238A structure is the well-defined density corresponding to the hydrated form (HDPR) of the purine riboside inhibitor within the mutant active site. The alanine mutant has catalyzed the hydration of PR on C-6, similarly to what occurs in crystals of wild-type ADA−PR complexes (Wilson et al., 1991). This result suggests that H238A, despite its low catalytic activity, is able to catalyze the deprotonation of the metal-bound water and formation of the hydroxylate during the crystallization process. Thus, these data indicate that His 238 is not required for formation of the catalytic hydroxylate and cannot be the base required for the deamination reaction.

The nonhydrated inhibitor, PR, is clearly seen in the active site of the H238E mutant. The finding of PR in this structure agrees with the extremely low catalytic efficiency of this enzyme (4×10^{-6} lower than the wild-type). Refinement of the metal coordination sphere shows a spherical region of density in a position similar to the zinc-activated water molecule observed in the wild-type ADA−1-deazaadenosine complex. This was fit in the mutant structure as a water molecule and refined to a position 3.16 Å from the Oϵ1 of Glu 238, 3.11 Å from the C-6 of PR, and a very short distance of 1.51 Å from the zinc. This water molecule is shown as a ligand to the metal in the H238E active site shown in Figure 8.

In summary, these crystallographic results reveal that the two His 238 mutants sustained differences only in the active site but not in the overall tertiary structure, in agreement with our results from circular dichroism and fluorescence spectroscopy. A zinc atom is present in both mutants, as FAA spectroscopy already indicated. The nonhydrated form of purine riboside is bound in the H238E mutant active site, and the attacking water may be destabilized by Glu at position 238 compared to wild-type ADA. The H238A structure reveals a water adjacent to the Ala at position 238, and the inhibitor is bound in its hydrated form, HDPR. This result suggests that H238A is able to catalyze formation of the hydroxylate and thus eliminates His 238 from being the base in the reaction.

^{13}C NMR and ^{13}C−^{1}H HMQC Spectra of Purine Riboside Complexes with Wild-Type ADA and H238A. To examine the ability of H238A to catalyze the hydration on C-6 of purine riboside, the ^{13}C NMR spectra of purine riboside complexes of H238A and wild-type ADA were obtained. Figure 9 shows the ^{13}C NMR spectra of 6-^{13}C purine riboside free in solution (A), bound in its complex with wild-type

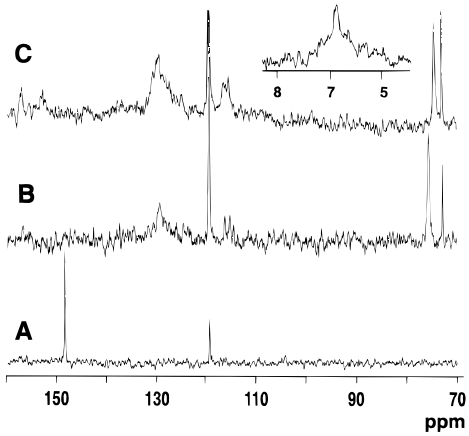

FIGURE 9: ^{13}C NMR spectra of purine riboside complexes with H238A and wild-type ADA: (A) 1 mM purine riboside, 500 transients; (B) 0.9 mM complex of purine riboside with wild-type ADA, 1400 transients; and (C) 0.7 mM complex of purine riboside with H238A ADA, 37 000 transients. (Insert) the HMQC ^1H NMR spectrum of the C-6 proton of hydrated purine riboside (HDPR) in its complex with H238A ADA, 464 transients.

ADA (B), and bound to H238A (C). The inset in the figure shows the proton spectrum from the HMQC experiment in which the single-bond correlation was established with the carbon resonance at 73.5 ppm. The attached proton is found at 6.84 ppm (the hump under the attached proton resonance arises from aromatic protons). The existence of a single proton *J*-coupled to the 73.5 ppm carbon resonance was confirmed by collecting an additional HMQC spectrum in the absence of carbon decoupling; this revealed a doublet with a J_{CH} value of ~200 Hz (data not shown).

In its complex with the wild-type enzyme, the 6-^{13}C carbon of HDPR resonates at 74.7 ppm and its attached proton at 7.03 ppm (data not shown). In its complex with H238A, the 6-^{13}C carbon of HDPR resonates at 73.7 ppm and its attached proton at 6.84 ppm. The sharp resonance at 71 ppm is due to glycerol remaining from the storage solution of the enzyme or from inadequate rinsing of the Centricon concentrator. The minor peaks at 153 and 157 ppm in the 1-D carbon spectrum of the H238A complex have not previously been seen in complexes of ADA or its mutants. However, HMQC experiments at those frequencies designed to detect a single proton fail to do so convincingly. These peaks probably arise from natural abundance arginine, guanidino, or tyrosine hydroxyl carbons detected only after the long collection time of the H238A experiment. Alternatively, they could represent a very minor amount of an alternate bound form or chance contaminants in the sample.

These results show that within the limits of experimental detection, the only form of purine riboside bound in the active site of H238A is the hydrated form. The values of both the carbon and proton chemical shifts of the bound hydrate are only minimally perturbed in the mutant in comparison to those found for the wild-type enzyme.

DISCUSSION

Effects of His 238 Mutations on ADA Structure. Substitution of an alanine or a glutamate for histidine 238 did not drastically alter ADA structure as judged by the elution characteristics of these mutants, their far- and near-UV circular dichroism spectra, fluorescence emission, crystal structures, and their substrate and inhibitor binding properties.

Table 3: Crystallographic, Data Collection, and Refinement Parameters for H238A and H238E ADA Crystal Structures

	H238A	H238E
unit cell parameters	$a = 99.14$ Å $b = 93.94$ Å $c = 71.98$ Å $\beta = 126.92°$	$a = 99.11$ Å $b = 93.81$ Å $c = 72.10$ Å $\beta = 126.83°$
unique/observations	22 029/71 281	21 992/51 632
R_{merge} (%)	5.2	5.8
reflections used in refinement	18 931	18 233
R_{cryst} (%)	20.3	20.3
rms bond deviation from ideality (Å)	0.017	0.014
rms angle deviation from ideality (deg)	1.98	1.78

The arginine mutation, while not perturbing the α-helices, β-sheets, or active site geometry, resulted in some localized tertiary structural differences, as the near-UV circular dichroism and tryptophan emission fluorescence spectra show. These localized differences may explain why the Arg 238 mutant failed to crystallize under conditions identical with those used with the Ala and Glu mutants.

Even though the fluorescence spectrum of H238R is quenched by approximately 25% relative to that of the wild-type and has a maximum at 333 vs 328 nm, it does not resemble the emission from guanidinium chloride-unfolded ADA, which has a maximum at 349 nm and is quenched by 60−70% (data not shown). This observation rules out global unfolding of the mutant as the cause of the spectral changes. Instead, the H238R fluorescence resembles the spectrum of calf ADA complexed to adenosine or adenosine analogs (Porter & Spector, 1992). Binding of these substrates to ADA causes the enzyme's tryptophan fluorescence emission to become quenched by 25−27% and the maximum to be slightly red-shifted.

Molecular modeling of an arginine at position 238 of ADA reveals that its side chain can rotate to within 6 Å of Trp 272, one of the two tryptophans located within 11 Å of the active site. This rotation brings Arg 238 in close contact with another aromatic residue, Tyr 240. If the bulky arginine cannot be accommodated in the ADA active site and must rotate, it may move, repositioning Tyr 240, whose near-UV CD signal would change. In addition, such a rotation would reorient Trp 272, altering its near-UV CD signal and quenching its fluorescence emission. Since Trp 272 is within 11 Å of the active site, it may be one of the components of the emission which become quenched upon binding of substrate or substrate analogs to the wild-type enzyme. Consequently, as a result of the Arg 238 rotation, the changes in the vicinity of Trp 272 may parallel those which occur upon ligand binding, causing the mutant fluorescence spectrum to become as quenched as the wild-type emission is upon ligand binding.

Effects of His 238 Mutations on Substrate and Inhibitor Binding. Replacement of His 238 by an acidic glutamate or a bulky arginine did not affect the enzyme's affinity for adenosine. Because of the low but measurable catalytic activity of H238R, inhibition studies could be carried out, and these showed that the arginine causes little or no change in the K_i values for PR and N^6MA, two competitive inhibitors of the enzyme. These results are consistent with structural information on the absence of bonding interactions between residue 238 and the substrate (Wilson et al., 1991).

Nevertheless, a 20-fold increase in the affinity of H238A for adenosine was observed with this mutant. This result was surprising, since no contact between His 238 and adenosine was predicted from the crystal structures (Wilson et al., 1991; Wilson & Quiocho, 1993 1994). Calculation of the distance between Nϵ2 of the histidine and N-6 of the substrate from the 1-deazaadenosine structure shows it to be 3.8 Å, too far for a hydrogen bond to form. However, Kurz et al. (1992) have pointed out that there must be an interaction between the 6-NH_2 substituent and ADA since 1-deazaadenosine (N-1 replaced by a carbon) is bound 100-fold more tightly by the enzyme than 1-deazapurine riboside (both N-1 and N-6 replaced by carbon atoms). The increased affinity for substrate by H238A was corroborated by the 10-fold lower K_i value of N^6-methyladenosine, an adenosine analog and weak substrate of ADA [K_m of 5 μM, k_{cat} of 0.3 s^{-1} (Porter & Spector, 1993)], as well as a competitive inhibitor of the enzyme. A 3-fold reduction in substrate affinity and 1000-fold drop in k_{cat}/K_m was observed for a similar H238A mutant in human ADA (Bhaumik et al., 1993). These combined results suggest that His 238 does not function in catalysis only by lowering the activation barrier to the transition state through hydroxylate charge stabilization (*vide infra*) but also by raising the energy of the enzyme−substrate complex.

Interestingly, an alanine mutation of Glu 104 (the primary catalytic residue) in cytidine deaminase results in a 10^8 reduction in k_{cat} and also a 30-fold reduction in K_m (Carlow et al., 1995). Since Glu 104 was thought to be engaged in two short hydrogen bonds with the altered substrate of this deaminase in the transition state (Betts et al., 1994), this increased substrate affinity of the Ala 104 mutant was unexpected. In fact, there seems to be a wealth of residues implicated in catalysis but not in substrate binding which, when mutated to alanine, exhibit higher affinities for substrate. Some histidines which belong to this group are His 372 in alkaline phosphatase (10-fold lower k_{cat} and 30-fold lower K_m; Xu et al., 1994) and His 64 in carbonic anhydrase (40-fold lower K_m and 70-fold lower k_{cat}; Liang et al., 1993), both zinc-utilizing enzymes.

One possible reason why substrate binding is improved when a catalytic histidine in ADA is replaced by alanine may be the removal of steric constraints. Eliminating histidine from the ADA active site and replacing it by alanine and a water molecule frees up space in the vicinity of C-6 of the purine ring, perhaps allowing substrate to bind more favorably. This theory would explain the lower K_m value for adenosine, which bears a C-6 amino group, and the lower K_i value for N^6MA, with its C-6 methylamino group. In the case of an inhibitor like PR, which lacks a C-6 substituent, binding may be too loose in the more spacious mutant active site; consequently PR becomes a poorer inhibitor with respect to adenosine in the Ala 238 mutant compared to the wild-type enzyme.

A second possibility is that His 238 may constrain the substrate, thus destabilizing it; removal of this residue would then result in better binding. Weiss et al. (1987) and Jones et al. (1989) have both suggested that the ADA substrate must be distorted during reaction in order for N-1 to become protonated and aromaticity of the purine ring to be decreased. The various wild-type and mutant ADA structures do not show any obvious distortion in substrate/inhibitor purine rings (Sideraki et al., 1996; Wilson et al., 1991). Moreover, the electron density of the purine ring is reduced by the engagement of all purine nitrogen lone pairs in hydrogen bonds. It is interesting, however, to note that, of all the residues in ADA structures, His 238 and Asp 295 are the only ones in high-energy, disallowed conformations (Wilson, 1996). This observation could mean that they are strained in their effort to maintain the substrate in an unfavorable conformation. Alternatively, this phenomenon may be a consequence of the specific electrostatic and hydrogen-bonding interactions between His 238 and Asp 295 and between Asp 295 and the zinc. Nevertheless, if His 238 constrains the substrate, and its absence results in tighter binding, it is difficult to rationalize the K_m values observed with H238E and H238R, which are not different from those of wild-type ADA.

Effects of His 238 Mutations on the Catalytic Efficiency of ADA. As more crystal structures of the ADA enzyme complexed to ground-state or transition-state analogs became available, a number of proposals were put forth regarding the role of His 238 in the reaction mechanism. Thus, this residue was initially proposed to orient and stabilize the incipient hydroxylate, formed by the action of Asp 295 (Wilson et al., 1991). Its role was later modified to be that of a general base, creating the hydroxylate from the zinc-bound water (Wilson & Quiocho, 1993). It was also suggested that His 238 may be the origin of the leaving group proton, despite the residue's long distance from the C-6 amino group; this proposal assigned an additional general acid function to this amino acid (Wilson & Quiocho, 1993).

Our objective in mutating His 238 was to elucidate the function of this histidine in the reaction. To this end, a neutral, apolar amino acid (Ala), an acidic, polar amino acid (Glu), and a basic, polar amino acid (Arg) were used as substitutions of His 238. The steady-state kinetic parameters reveal that the three mutations of histidine 238 reduce, but do not abolish, ADA catalytic activity. This result, combined with the finding of the hydrated form of PR in the H238A active site by both crystallography and NMR spectroscopy, clearly shows that histidine 238 is *not the base* which creates the attacking OH group. However, His 238 is important to the reaction, as the low k_{cat}/K_m values of the mutants show.

Of the three mutants, H238E exhibits the lowest activity (k_{cat}/K_m only 4×10^{-6} that of the wild-type), a result which suggests that the negative charge on the glutamate is greatly detrimental to catalysis. By comparison, an uncharged (Ala-water) or positively charged (Arg) residue at position 238 is more easily tolerated. The H238E crystal structure shows that this mutant is unable to catalyze the hydration of PR to form HDPR. An acidic residue at position 238 may result in destabilization of the zinc-coordinated hydroxylate or possibly interfere with its formation. Thus, even though His 238 may not be the base, its presence promotes deprotonation of the zinc-water. These results support an electrostatic role for His 238 in stabilizing the developing negative charge on the hydroxylate.

If electrostatic stabilization of the OH^- is the key function of His 238, an arginine residue at 238 with its positive charge should result in little loss of catalytic activity. In agreement with this prediction, the Arg mutant has a 170-fold higher turnover rate compared to the Glu 238 mutant. The favorable electrostatic effect of the basic arginine, however, may be offset by its reorientation within the active site. Conse-

quently, any contribution of the guanidinium positive charge to hydroxylate stabilization is lost. In addition, if His 238 is indeed the donor of the leaving group proton, the high pK_a of the Arg side chain precludes its function as a general acid. This mutant has therefore only 0.06% of the wild-type catalytic efficiency.

The importance of a positive charge at position 238 is underscored by pH studies of the kinetic behavior of H238A. In this mutant, which is normally 500-fold less active than wild-type ADA, both the k_{cat} and k_{cat}/K_m values *increase* at pH 5.5 relative to pH 7.0, opposite from wild-type behavior (Table 2). As the crystal structure shows, a water is found next to the engineered alanine at this position. At acidic pH values, a hydronium ion can replace this water in the H238A active site. The positive charge on the hydronium ion can stabilize the incipient hydroxylate negative charge. In addition, a proton from the hydronium could be transferred to the leaving group, allowing elimination to occur and completion of the reaction. The altered pH profiles for the reaction catalyzed by H238A also suggest that the rate-determining step has now changed. This is not surprising, since, in the absence of His 238, formation of the hydroxylate and/or collapse of the tetrahedral intermediate into products may be the most difficult steps.

His 238 could be stabilizing the negative hydroxylate charge directly or indirectly. In another zinc-utilizing enzyme, alkaline phosphatase, His 372 hydrogen-bonds with one of the carboxyl oxygens of Asp 327, a bidentate ligand to the zinc. In the wild-type enzyme, His 372 is thought to neutralize the negative charge of the Asp 327, which in turn becomes a worse electron donor to the zinc. That makes the metal more electrophilic, and the metal-bound water is rendered a better nucleophile. An alanine mutant of this histidine had a 10-fold lower hydrolysis activity and 30-fold higher substrate affinity compared to wild-type (Xu et al., 1994). In the H372A mutant the aspartate charge is not neutralized, and the water is a worse nucleophile (i.e., its pK_a is higher); thus, reaction slows down. We may be witnessing a very similar effect with our H238A mutant. With an alanine in place of a histidine, the electrostatic effects are lost (unless the water found next to Ala 238 becomes charged, as in acidic pH values) and the water is less polarized because it is bonded to the zinc less tightly. If this is true, then we would expect the Zn−water bond to be longer and, by inference, the zinc−Asp 295 bond to be shorter (stronger) in the H238A structure than it is in the wild-type. This is in fact true. The zinc−Asp 295 distance in H238A is 2.1 Å versus the wild-type 2.4 Å. In H238E, where there is an added negative charge in the immediate vicinity of Asp 295, this distance drops to 2 Å. None of the other histidine ligand−zinc distances have been affected.

Since HDPR cannot eliminate its leaving group (a hydrogen), the present data do not allow us to distinguish between a role of the histidine in charge stabilization of the hydroxylate or in protonation of the leaving group. Nevertheless, whether His 238 acts as a general acid or merely has an electrostatic effect (or performs both functions), this study clearly eliminates His 238 from being the base required to bring about the first part of the ADA-mediated reaction.

REFERENCES

Adler, A. J., Greenfield, N. J., & Fasman, G. D. (1973) in *Methods in Enzymology* (Hirs, C. H. W., & Timasheff, S. N., Eds.) Vol. 27, pp 675−735, Academic Press, New York.

Betts, L., Xiang, S., Short, S., Wolfenden, R., & Carter, C. W., Jr. (1994) *J. Mol. Biol. 235*, 635−656.

Bhaumik, D., Medin, J., Gathy, K., & Coleman, M. S. (1993) *J. Biol. Chem. 268*, 5464−5470.

Bradford, M. (1976) *Anal. Biochem 72*, 248−254.

Carlow, D. A., Smith, A. A., Yang, C. C., Short, S. A., & Wolfenden, R. (1995) *Biochemistry 34*, 4220−4224.

Chang, Z., Nygaard, P., Chinault, A. C., & Kellems, R. E. (1991) *Biochemistry 30*, 2273−2280.

Freskard, P., Martensson, L., Jonasson, P., Jonsson, B., & Carlsson, U. (1994) *Biochemistry 33*, 14281−14288

Frick, L., Neela, J. P., & Wolfenden, R. (1987) *Bioorg. Chem. 15*, 100−108.

Jones, W., Kurz, L. C., & Wolfenden, R. *Biochemistry 28*, 1242−1247.

Kati, W. M., & Wolfenden, R. (1989) *Science 243*, 1591−1593.

Kline, P. C., & Schramm, V. L. (1994) *J. Biol. Chem. 269*, 22385−22390.

Kraulis, P. J. (1991) *J. Appl. Crystallogr. 24*, 946−950.

Kunkel, T. A., Roberts, J. D., & Zakour, R. A. (1987) *Methods Enzymol. 154*, 367−382.

Kurz, L. C., & Frieden, C. (1983) *Biochemistry 22*, 382−389.

Kurz, L. C., & Frieden, C. (1987) *Biochemistry 26*, 8450−8457.

Kurz, L. C., LaZard, D., & Frieden, C. (1985) *Biochemistry 24*, 1342−1347.

Kurz, L. C., Moix, L., Riley, M. C., & Frieden, C. (1992) *Biochemistry 31*, 39−48.

Laemmli, U. K. (1970) *Nature 227*, 680−685.

Liang, Z., Jonsson, B., & Lindskog, S. (1993) *Biochim. Biophys. Acta 1203*, 142−145.

Mohamedali, K. A., Kurz, L. C., & Rudolph, F. B. (1996) *Biochemistry 35*, 1672−1680.

Philips, A. V., Coleman, M. S., Maskos, K., & Barkley, M. D. (1989) *Biochemistry 28*, 2040−2050.

Porter, D. J. T., & Spector, T. (1993), *J. Biol. Chem. 268*, 2480−2485.

Sideraki, V., Mohamedali, K. A., Wilson, D. K., Chang, Z., Kellems, R. E., Quiocho, F. A., & Rudolph, F. B. (1996) *Biochemistry 35*, 7862−7872.

Vuilleumier, S., Sancho, J., Loewenthal, R. and Fersht, A. R. (1993) *Biochemistry 32*, 10303−10313.

Weiss, P. M., Cook, P. F., Hermes, J. D., & Cleland, W. W. (1987) *Biochemistry 26*, 7378−7384.

Wilson, D. K. (1996) Ph.D. Thesis, Baylor College of Medicine, Houston, TX.

Wilson, D. K., & Quiocho, F. A. (1993) *Biochemistry 32*, 1689−1693.

Wilson, D. K., & Quiocho, F. A. (1994) *Struct. Biol. 1*, 691−694.

Wilson, D. K., Rudolph, F. B., & Quiocho, F. A. (1991) *Science 252*, 1278−1284.

Wolfenden, R. (1969) *Biochemistry 8*, 2409−2412.

Wolfenden, R., Wentworth, D. F., & Mitchell, G. N. (1977) *Biochemistry 16*, 5071−5077.

Xu, X., Qin, X., & Kantrowitz, E. R. (1994) *Biochemistry 33*, 2279−2284.

Yeung, C., Ingolia, D. E., Roth, D. B., Shoemaker, C., Al-Ubaidi, M. R., Yen, J., Ching, C., Bobonis, C., Kaufman, R. J., & Kellems, R. E. (1985) *J. Biol. Chem. 260*, 10299−10307.

Zielke, C. L., & Suelter, C. H. (1971) in *The Enzymes* (Boyer, P. D., Ed.) Vol. 4, pp 47−48, Academic Press, New York.

BI961427E